European Journal of Neuroscience, Vol. 12, pp. 1635–1646, 2000

Dendritic L-type calcium currents in mouse spinal motoneurons: implications for bistability

K. P. Carlin,[2] K. E. Jones,[2] Z. Jiang,[2] L. M. Jordan[2] and R. M. Brownstone[1,2]
Departments of [1]Surgery and [2]Physiology, University of Manitoba, 730 William Avenue, Winnipeg, MB, Canada R3E 3J7

Keywords: dihydropyridines, locomotion, plateau potential, spinal cord model

Abstract

The intrinsic properties of mammalian spinal motoneurons provide them with the capability to produce high rates of sustained firing in response to transient inputs (bistability). Even though it has been suggested that a persistent dendritic calcium current is responsible for the depolarizing drive underlying this firing property, such a current has not been demonstrated in these cells. In this study, calcium currents are recorded from functionally mature mouse spinal motoneurons using somatic whole-cell patch-clamp techniques. Under these conditions a component of the current demonstrated kinetics consistent with a current originating at a site spatially segregated from the soma. In response to step commands this component was seen as a late-onset, low amplitude persistent current whilst in response to depolarizing–repolarizing ramp commands a low voltage clockwise current hysteresis was recorded. Simulations using a neuromorphic motoneuron model could reproduce these currents only if a noninactivating calcium conductance was placed in the dendritic compartments. Pharmacological studies demonstrated that both the late-onset and hysteretic currents demonstrated sensitivity to both dihydropyridines and the L-channel activator FPL-64176. Furthermore, the α_{1D} subunits of L-type calcium channels were immunohistochemically demonstrated on motoneuronal dendrites. It is concluded that there are dendritically located L-type channels in mammalian motoneurons capable of mediating a persistent depolarizing drive to the soma and which probably mediate the bistable behaviour of these cells.

Introduction

It has been demonstrated in cat motoneurons that the prolonged discharges seen following brief synaptic inputs (Hultborn *et al*., 1975) result not from continued activity in premotoneuronal circuits but rather from intrinsic properties of the motoneurons themselves (Hounsgaard *et al*., 1984; Crone *et al*., 1988; Lee & Heckman, 1996). This membrane property (plateau potential) provides two stable membrane potentials, one a resting potential and the other a potential which produces sustained firing (i.e. bistability). This property is thought to be important for the production of motoneuron output during fictive locomotion (Brownstone *et al*., 1994), as well as for the maintenance of posture in intact, awake mammals (Eken & Kiehn, 1989), possibly including humans (Kiehn & Eken, 1997). In the cat, it was surmised that a voltage-dependent 'persistent' calcium current underlies this property (Schwindt & Crill, 1980). Later, noninactivating L-type calcium channels were shown to mediate this current in turtle motoneurons (Hounsgaard & Kiehn, 1989).

Is an L-type current also responsible for plateau potentials and bistability in mammalian motoneurons? Unfortunately, pharmacological investigations of these currents is difficult *in vivo*, and calcium-mediated bistability has not been demonstrated *in vitro*. There are probably for two reasons for the latter. Firstly, most investigators studying mammalian spinal motoneurons *in vitro* use neonatal animals (e.g. Ziskind-Conhaim, 1988; Takahashi & Berger, 1990; MacLean *et al*., 1997). As both known types of L-type channels (class C and class D) show developmental changes during the postnatal period in mice (Jiang *et al*., 1999a), younger motoneurons may not have the ability to produce plateau potentials. Secondly, there is evidence from turtle (Hounsgaard & Kiehn, 1993) and cat motoneurons (Lee & Heckman, 1996; 1998b; Bennett *et al*., 1998) and from modelling studies (Booth *et al*., 1997; Gutman, 1991) that these currents originate in the dendrites. Therefore, the use of culture techniques that limit dendritic morphology may preclude their demonstration (e.g. Mynlieff & Beam, 1992). To overcome these problems, spinal cord slices from animals which have 'functionally mature' motor systems (they are able to weight-bear and walk; Jiang *et al*., 1999b) were used in this study. At this stage, L-type channels contribute to a rhythmic motor output elicited in *in vitro* spinal cords (Jiang *et al*., 1999a).

The hypothesis that mammalian spinal motoneurons have noninactivating dendritic calcium currents was then examined. As these conductances would be electrotonically distal to the somatic recording site, they would not be adequately voltage clamped. In this situation, the presence of dendritic conductances would be seen as currents with delayed activation in response to constant voltage commands (Müller & Lux, 1993) and as producing a clockwise hysteresis in response to voltage ramp commands (Svirskis & Hounsgaard, 1997; Lee & Heckman, 1998b). Such currents are demonstrated in this study. The pharmacology of this current and the immunohistochemical demonstration of L-type calcium channels on motoneuronal dendrites lead to the suggestion that the presence of dendritic L-type calcium channels is a phylogenetically conserved characteristic of spinal motoneurons. The kinetics and subcellular location of these channels make them ideal candidates to mediate the expression of bistability in mammalian motoneurons.

Correspondence: R.M. Brownstone, as above.
E-mail: rob@scrc.umanitoba.ca

Received 26 October 1999, revised 1 February 2000, accepted 3 February 2000

Materials and methods

Slice preparation, electrophysiology, solutions and chemicals

All animals [postnatal days (P) 8–15] Balb/C mice) were anaesthetized, and the experimental procedures were approved by the University of Manitoba Animal Care Committee and conformed to the standards of the Canadian Council of Animal Care. All chemicals were obtained from Sigma (St Louis, USA) unless otherwise specified.

The isolation of the spinal cord, preparation of slices, whole-cell patch-clamp recordings, and solutions and chemicals were as described in the companion paper (Carlin *et al*., 2000).

Motoneurons were identified as the largest cells (> 20 μm mean diameter; McHanwell & Biscoe, 1981; Takahashi, 1990) in the ventral horn (Gao & Ziskind-Conhaim, 1998; Jonas *et al*., 1998; Carlin *et al*. 2000; but see Thurbon *et al*., 1998). Voltage step protocols are indicated in the text. The standard voltage ramp protocol consisted of stepping the potential to –120 mV for ≈ 1 s from a holding potential of –60 mV. The potential was then ramped to +60 mV and back to –120 mV over a period of 20 s. Such slow ramps minimize the effects of transient currents.

Modelling

The three-dimensional morphology of a cat lumbar spinal motoneuron (courtesy of R.E. Burke) was incorporated into the NEURON simulation environment (Hines & Carnevale, 1997). A morphometric and electrotonic analysis of this cell has previously been published (FR MG MN 43/5: Cullheim *et al*., 1987a, b; Fleshman *et al*., 1988). The passive parameters assigned to the model motoneuron were membrane resistance, $R_m = 0.25\ k\Omega\text{-}cm^2$ in the soma and $11\ k\Omega\text{-}cm^2$ in the dendrites, membrane capacitance, $C_m = 1\ \mu F/cm^2$, and access resistance (R_a) $= 70\ \Omega$-cm (see Fleshman *et al*., 1988).

Voltage-dependent conductances were modelled using Hodgkin–Huxley formalism. These conductances consisted of two different types of Ca^{2+} channels: a transient high-voltage-activated N-like conductance and a persistent L-like conductance. The parameters describing the kinetics of these conductances were adapted from Avery & Johnston (1996) and Booth *et al*. (1997) and are given in Table 1.

The general form of the equations describing these conductances was:

$$I = g_{max} m^x h^y (V_m - E_{rev})$$

$$m' \text{ (or } h') = [m_\infty(V_m) - m]/\tau_m$$

$$m_\infty \text{ (or } h_\infty) = 1/\{1 + \exp[(V_m - \theta_m)/\kappa_m]\}$$

where V_m is the membrane potential, m' is the rate of change of m (i.e. activation or h, inactivation) and m_∞ is the steady-state value for activation.

The density of the maximal conductance, g_{max}, for the channels depended on the localization of the channels on the dendrite or soma. The differential equations were solved using the backward Euler method with a time step of 0.025 ms. Voltage clamp simulations were performed using similar protocols to the *in vitro* electrophysiology.

Immunohistochemistry

Transcardial perfusion was performed with cold (4 °C) prefixative solution consisting of 50 mM sodium phosphate buffer, 0.9% saline, 0.1% sodium nitrite and 0.01% heparin. This was followed by perfusion with cold 4% paraformaldehyde, 0.2 M L-lysine, 0.02 M Na-M-periodate solution containing 0.1 M phosphate buffer, pH 7.4. The lumbar spinal cords were harvested and postfixed in this same fixative overnight and then placed in cryoprotectant consisting of 10% sucrose in 50 mM phosphate buffer. The tissue was blocked in OCT embedding compound (Miles, Elkhart, IN, USA) and sectioned transversely on a cryostat to a thickness of 20 μm, then thaw-mounted onto gelatin-coated glass slides. Slides were washed overnight in 50 mM Tris-HCl-buffered saline prior to processing. All dilutions and washes were performed in Tris-HCl-buffered saline and incubations included 1% normal horse serum (Sigma).

Polyclonal rabbit anti-rat α1d subunit antibody (Alamone Labs, Jerusalem) was used to label Class D L-type Ca^{2+} channels. Sections were incubated in anti-α1d subunit diluted 1 : 500 for 3 days at 4 °C. Sections were washed for 3 × 20 min and all slides were incubated for 3 h with donkey anti-rabbit cy3 (Jackson Labs, West Grove, PA, USA) diluted 1 : 250. The sections were then washed for 10 min in Tris-HCl-buffered saline, followed by 2 × 10 minute washes in 50 mM Tris-HCl buffer, and coverslipped using Vectashield (Vector Labs, Burlingame, CA, USA). Control procedures were done using sections processed as described above with (a) omission of the primary antibody, and (b) absorption of the peptide. A Molecular Dynamics confocal scanning laser microscope equipped with an argon laser was then used to generate individual optical sections, which were then volume-rendered and presented as look-through projections using Image Space software interpolation on a Silicon Graphics Indigo computer.

TABLE 1 Parameters used for modelling calcium conductances in somatic and dendritic compartments

Ca^{2+} conductance	g_{max} (S/cm^2)	x	y	E_{rev} (mV)	τ_m (ms)	τ_h (ms)	θ_m (mV)	θ_h (mV)	κ_m (mV)	κ_h (mV)
N-like										
Soma	0.05	2	1	60	4	40	–30	–45	–5	5
Dendrites	0.002									
L-like HVA										
Soma	0.01	1	0	60	20		–10		–6	
Dendrites	0.0003									
L-like LVA										
Soma	0.01	1	0	60	20		–30		–6	
Dendrites	0.0003									

g_{max}, maximum conductance; m, activation state; h, inactivation state; E_{rev}, reversal potential; τ_m, activation time constant; τ_h, inactivation time constant; θ_m, half-activation voltage; θ_h, half-inactivation voltage; κ_m, slope of activation curve; κ_h, slope of inactivation curve; HVA, high-voltage-activated; LVA, low-voltage-activated.

Results

Late-onset, persistent currents

Calcium currents were elicited in motoneurons in 150–200 μm mature mouse spinal cord slices using whole-cell patch-clamp techniques with intra- and extracellular solutions designed to eliminate sodium and potassium currents. The high-voltage-activated currents in these cells have components of L-, N-, P/Q- and R-type conductances (Carlin *et al*. 2000). In a number of cells the presence of a sustained late-onset conductance could be seen (Fig. 1A). This conductance could be identified by either an inflection point in the current trace during a single voltage step or as a current with delayed onset (Hirst & McLachlan, 1986; Streit & Lux, 1989; Müller & Lux, 1993; Destexhe *et al*., 1998). The occurrence of both of these events was increased with the use of higher concentrations of calcium in the recording solution (Fig. 2A). Both an inflection point and a current with delayed onset are consistent with a lack of voltage control (space

clamp) of an inward conductance that is electrotonically relatively distant. These currents, referred to here as 'late currents', were seen in 37 out of 46 motoneurons (80%; 2 mM calcium, 500 ms × 2 mV increments), where the delay to activation of this current was variable and depended on the holding potential, the amplitude of the voltage step, and the extracellular calcium concentration (Fig. 2A). They were blocked by extracellular cadmium (not shown). The inability of the somatic repolarization to rapidly deactivate this conductance also supports a distal origin for this current (large tail currents in Fig. 1A).

In turtle (Svirskis & Hounsgaard, 1998) and cat (Lee & Heckman, 1998a, b) motoneurons that have plateau potentials, as well as in plateau potential modelling studies (Booth *et al.*, 1997), a hysteresis is seen in the current-voltage (*I–V*) relationship in response to slow depolarizing and hyperpolarizing ramp voltage commands. In other words, there is a region on this *I–V* relationship where the inward current during the hyperpolarizing ramp is greater than that seen during the depolarizing ramp. Such slow ramp commands were applied to mouse motoneurons in this study, and produced a region of hysteresis in 17 out of 22 (77%) motoneurons. A typical example is shown in Fig. 1B, where there was a relatively slowly increasing inward current on the depolarizing ramp, followed by an inflection point and a more steeply activating inward current. On the hyperpolarsing limb of the ramp, this latter inward current was reduced in amplitude and additional inward current appeared at more hyperpolarized voltages. When the figure was manipulated by overlaying the ascending and descending ramps as illustrated in Fig. 1C, this additional current at hyperpolarized voltages led to a clockwise hysteresis, as indicated by the arrows. An inflection point was clearly seen during the hyperpolarizing ramp, thus producing a 'double hump.' Note that this inward calcium current deactivated at a more hyperpolarized point than the potential at which it activated on the ascending limb. This current hysteresis will subsequently be referred to as the hysteretic current. In some cells in which hysteretic currents were not readily evident in 1 mM calcium, they could be demonstrated following the application of additional calcium to the bath (e.g. Fig. 2B). This is a similar finding to that shown with the late currents (Fig. 2A).

It was noted that in all cells with late-onset persistent currents, an hysteretic *I–V* relation was seen. Experiments were undertaken in 19 cells using both ramp (–120 to +60 to –120 mV over 20 s) and

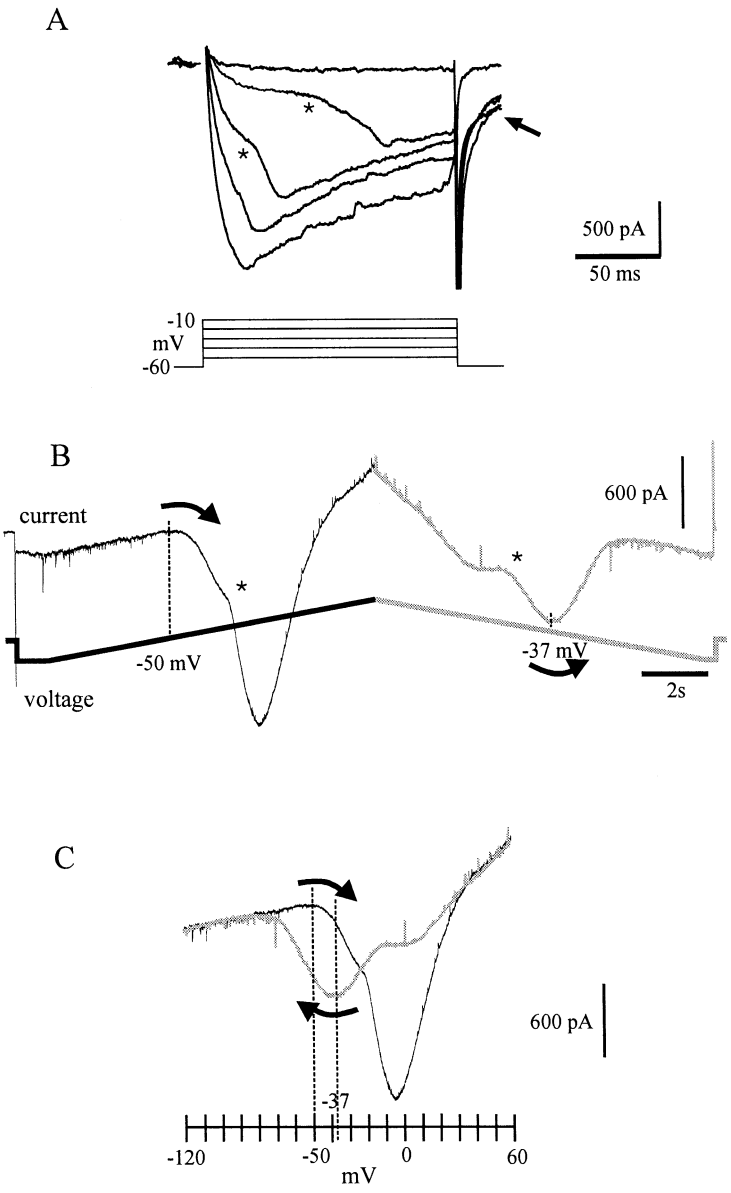

FIG. 1. Both late-onset and hysteretic calcium currents can be seen in motoneurons. (A) An example of late-onset, low amplitude persistent currents seen in a postnatal day 12 (P12) motoneuron. The late-onset currents (*) were activated earlier and more rapidly with increasing voltage commands. Voltage steps of 150 ms duration from –60 to –10 mV in 10 mV increments (whole-cell capacitance (WCC) 243 pF, input resistance (R_i) 101 MΩ, access resistance (R_a) 8.1 MΩ. Note the large tail currents (arrow). (B) Calcium currents elicited from a P10 motoneuron in response to a slow voltage ramp command (from –120 mV to +60 mV to –120 mV over 20 s). Ascending limb of the ramp is black and the descending limb is grey. Inflection points indicated by asterisks (*) (WCC 213 pF, R_i 440 MΩ, R_a 10.8 MΩ). (C) Superimposing the mirror image of the hyperpolarizing current response (grey) onto the depolarizing current response (black) demonstrates a clockwise calcium current hysteresis (arrows as in B). The hysteresis was the result of additional inward current during the hyperpolarizing phase of the ramp which was not present during the depolarizing phase. The dotted lines mark the onset of the negative slope conductance on the ramp up, and the peak hysteretic current on the ramp down.

voltage step protocols (2 mV × 500 ms steps) in 2 mM calcium to examine the converse; that is, are late currents always seen if there are hysteretic currents? A hysteretic current was seen in 14 out of 19 (74%) cells; 13 of these had late currents and one did not. In the remaining five (26%) cells, neither hysteresis nor late currents were seen (Fig. 2C).

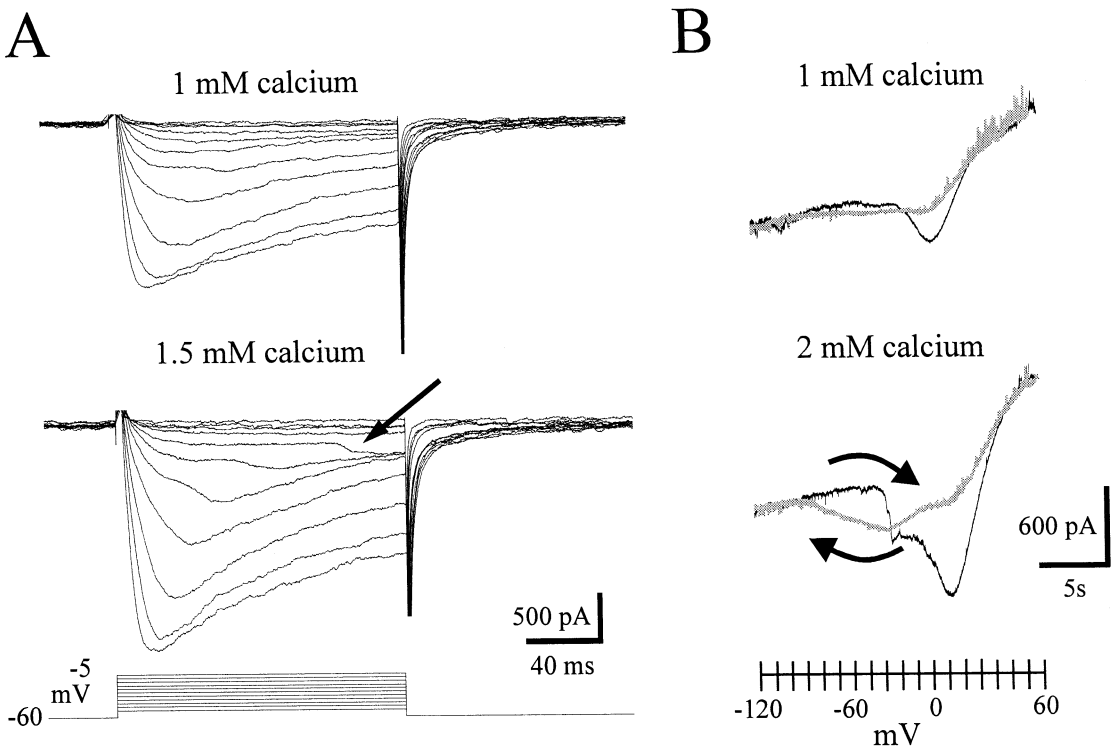

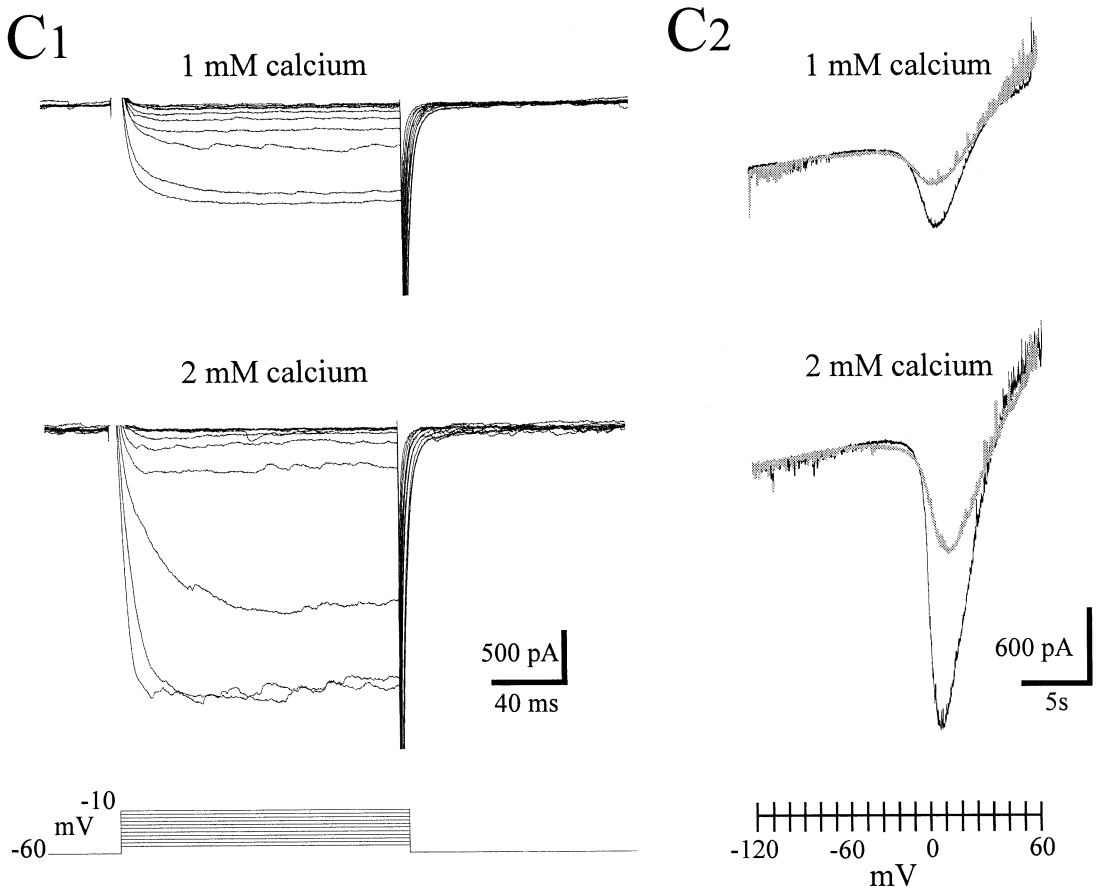

The voltage of activation of the channels mediating these currents cannot be determined from the present studies, which rely on the fact that the morphology of the cells precludes space clamp. Nevertheless, it was hypothesized that because the late currents were seen with small depolarizing commands, the voltage at which the negative slope conductance began in the voltage ramps (the 'apparent' activation voltage) should be more negative in the cells with hysteresis than in those without. This was found to be the case. Cells with hysteresis had an apparent activation voltage of -47 ± 8.6 mV (mean $\pm$ SD; $n = 14$), which was significantly more hyperpolarized than in the cells without hysteresis (-38 ± 3.8 mV; $n = 5$; t-test, $P < 0.05$).

Modelling of the late-onset and hysteretic currents

The hypothesized explanation for the late-onset and hysteretic currents was that they were due to calcium currents originating in the dendrites. To examine this further, a neuromorphic model was constructed using a three-dimensional reconstruction of a cat motoneuron (Cullheim *et al*., 1987a, b; Fleshman *et al*., 1988). Although the data are limited regarding the morphological and biophysical properties of mouse motoneurons, it is known that rat motoneurons are biophysically very similar to cat motoneurons (Thurbon *et al*., 1998). The cat motoneuron data was therefore used as a reasonable first approximation of a mouse motoneuron.

Sodium and potassium conductances were not included in the model. Three calcium conductances were modelled (Table 1 and Fig. 3) which differed in activation threshold [high- (HVA) vs. low-voltage-activated (LVA) L-type] and inactivation kinetics (L-type vs. N-type). The model was used to explore: (i) the effects of spatial segregation of the various calcium conductances on the production of late-onset and hysteretic currents; and (ii) the effects of voltage threshold and inactivation kinetics on the kinetics of the late and hysteretic currents. Each of the three conductances was uniformly distributed in either the somatic or the dendritic (distal to the third branch point) region of the modelled cell. The densities of the modelled calcium currents were adjusted to give peak current densities of the same magnitude as those seen in the experimental data. The model then simulated the experimental voltage clamp protocols using both step and ramp voltage commands.

During voltage step protocols, a late-onset current was seen only when a noninactivating current was placed in the dendrites (Fig. 3A). This could be modelled with either LVA or HVA properties but a qualitatively better match with experimental results was obtained with the LVA current (compare with Fig. 5Aii). Placement of an N-type conductance in the dendrites produced a slowing of their activation kinetics as expected, but did not lead to a sustained late-onset current. In addition, the deactivation of a distal conductance was slower than the deactivation of the more proximal conductances. This can be seen by the prolonged tail currents produced by both the HVA and to a greater extent by the LVA L-type conductances placed in the dendritic region (Fig. 3A, compare with Fig. 1A).

With ramp voltage commands, it was necessary to place the voltage-activated channels in the dendrites to obtain clockwise hysteresis (Fig. 3B). The difference between the hysteresis produced by the dendritically located LVA or HVA noninactivating currents was in the voltage of onset of the negative current slope. With the LVA channels (Fig. 3Bii), the apparent activation voltage was –45 mV whilst with the HVA channels the activation voltage was –14 mV. On combining an LVA L-type dendritic current with an HVA L-type somatic current, both the voltage steps and ramps produced results strikingly similar to those seen experimentally, including the late-onset current, the prolonged tail current and the clockwise hysteresis with two current peaks during the hyperpolarising ramp (e.g. compare Figs 1C and 3C). This lends support to the hypothesis that these late inward and hysteretic currents result from the activation of a noninactivating L-type conductance in the dendrites, possibly with a relatively low activation threshold.

Pharmacology of the late-onset and hysteretic currents

Cells displaying the late-onset currents were exposed to ω-conotoxin-GVIA (3–6 μM) to block N-type (Feldman *et al*., 1987), ω-agatoxin-TK (400 nM) to block P/Q-type (Teramoto *et al*., 1995) and nifedipine (20 μM) or nimodipine (10–20 μM) to block L-type calcium channels. The L-type calcium channel activator FPL-64176 (5.8 μM) was also used to confirm the contribution of L-type channels (Randall & Tsien, 1995). Cells were either incubated (30–70 min) in the blockers or had the blockers acutely applied.

To discriminate the effectiveness of each blocker on the late-onset currents, acute application experiments were undertaken. The late-onset currents were sensitive to both the dihydropyridines nifedipine and nimodipine (seven out of seven cells; Fig. 4A). The current inflections were completely ($n = 2$) or partially ($n = 1$) blocked by application of 20 μM nifedipine. Similarly, application of 10–20 μM nimodipine completely blocked ($n = 3$) or reduced ($n = 1$) the current inflections.

Because sensitivity to dihydropyridines is the hallmark of L-type calcium channels, these results indicate that at least part of the late-onset conductance is mediated through L-type channels. This possibility was further tested with the application of the potent L-type channel activator FPL-64176. Application of FPL-64176 (5.8 μM) to cells with the late-onset currents caused an enhancement of these currents (two out of two cells; Fig. 4B). In addition to the increased amplitude, this enhancement was characterized by reducing the somatic voltage at which the late current was first seen and by producing large slowly activating currents.

Similar effects of these drugs were seen with the ramp voltage commands. FPL-64176 not only had the expected effect of increasing the amplitude and shifting the peak inward current on the ascending ramp to the right, but it also increased the amplitude of the hysteretic current and delayed its deactivation, as can be seen during the hyperpolarizing ramp (two out of two cells; Fig. 4C). This current was blocked by nimodipine (20 μM; two out of two cells; Fig. 4C). Given that the apparent activation voltage is more hyperpolarized in cells

FIG. 2. Late-onset and hysteretic currents were seen in most but not all motoneurons, and were dependent on extracellular calcium. (A) Voltage steps of 150 ms duration from –60 to –5 mV in 5-mV increments in a P12 motoneuron (WCC 184 pF, R_i 214 MΩ, R_a 6.9 MΩ). After the addition of extra calcium (R_i increased to 305 MΩ), a late-onset inward current was seen (arrow) with a progressively shorter delay with increasing voltage commands. (B) Current responses to voltage ramp commands in a P13 motoneuron before and after the addition of 1 mM calcium (WCC 163 pF, R_i 350 MΩ in 2 mM calcium). The addition of extra calcium enhanced the hysteretic current. The black and grey current traces are as in Fig. 1. (C) In some cells, such as this P10 motoneuron (WCC 236 pF, R_i 447 MΩ, R_a 9.8 MΩ), neither the late-onset (C1) nor the hysteretic (C2) currents could be demonstrated, even after increasing the extracellular calcium concentration (R_i increased to 490 MΩ).

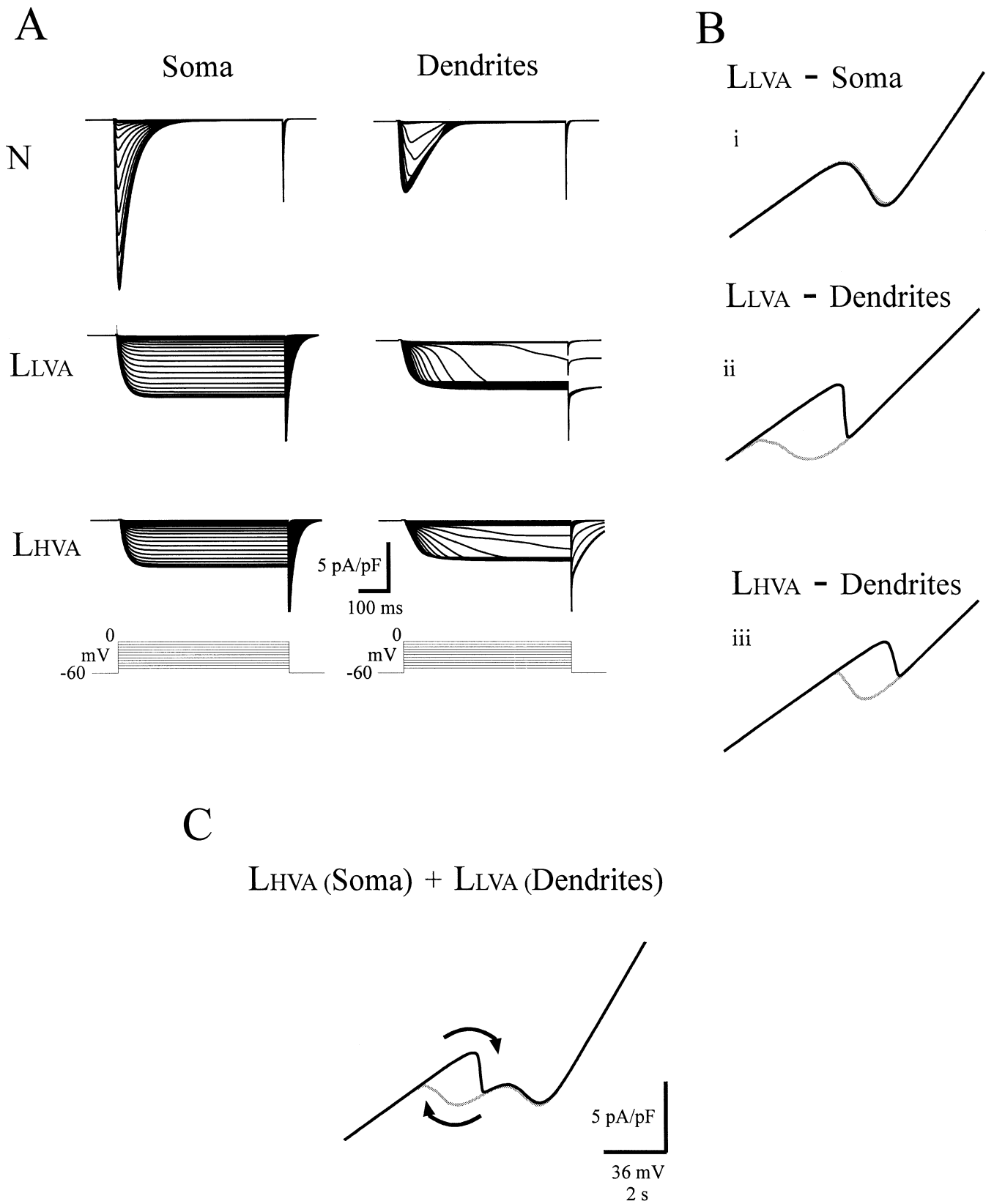

FIG. 3. The models containing dendritic L-type channels demonstrate currents similar to those seen experimentally. (A) Neither N-type currents in the soma or dendrites, nor L-type (LVA or HVA) currents in the soma resulted in late-onset currents. Such currents were seen only with L-type currents in the dendrites. Note the large, persistent tail currents with LVA L-type currents in the dendrites (middle row, right). (B) Similarly, hysteretic currents were seen only with L-type currents in the dendrites. Note that the placement of LVA L-type currents in the dendrites results in currents very similar to those seen experimentally, with a low voltage of onset and delayed deactivation on the downward ramp. (C) The inclusion of HVA L-type currents in the soma with the LVA L-type currents in the dendrites resulted in hysteretic currents very similar to those seen experimentally, including the 'double-hump' on the downward ramp.

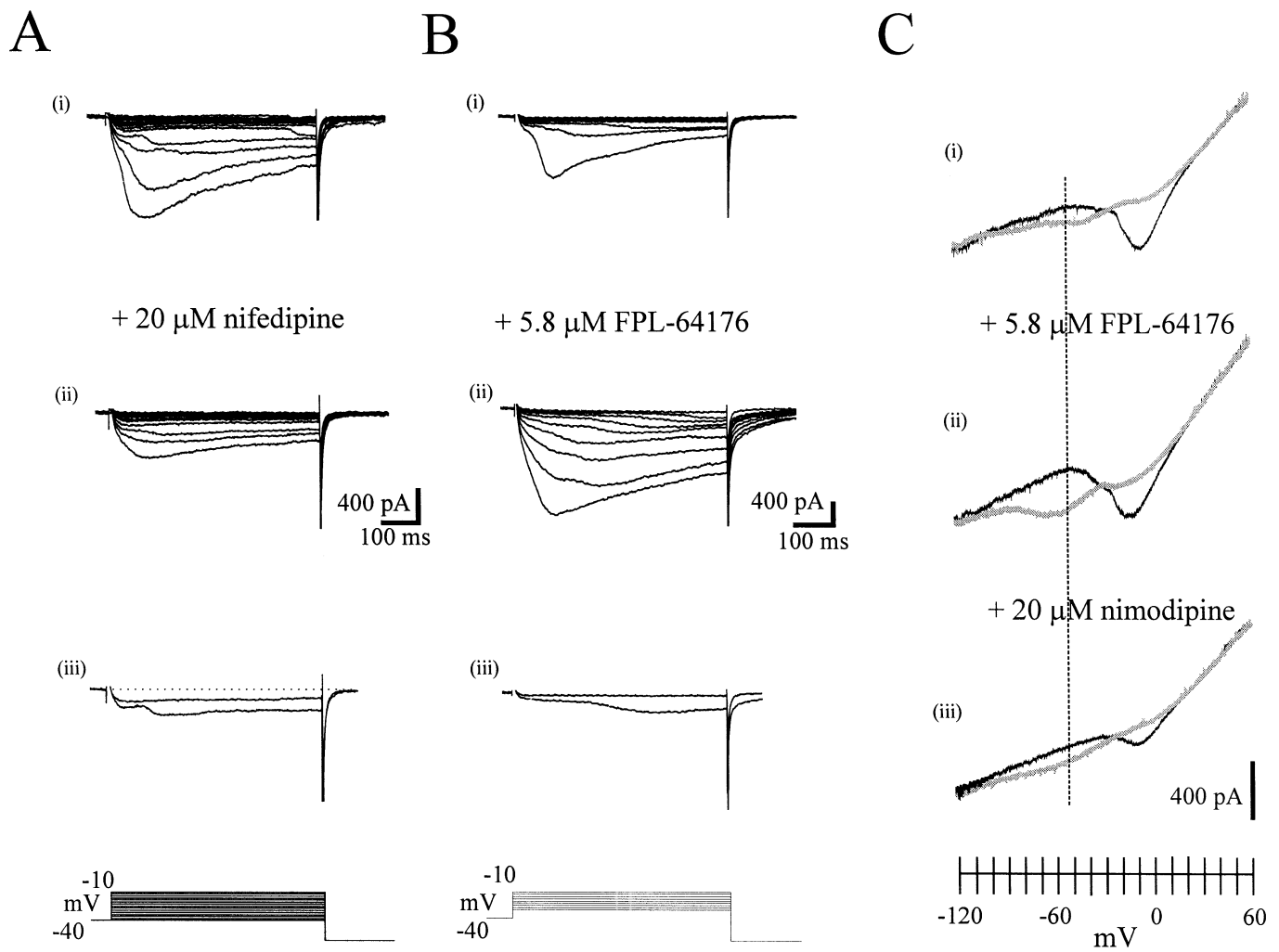

FIG. 4. The dendritic current is mediated by L-type calcium channels. (A) The late-onset currents seen in this P9 motoneuron in (i) 2 mM calcium were (ii) antagonized after application of nifedipine. (iii) The steps to –16 mV before and 13 min after the application of nifedipine were overlaid. (B) The late-onset currents seen in this P11 motoneuron were still present (i) ≈ 6 min after the addition of ω-agatoxin and ω-conotoxin and (ii) were enhanced after application of FPL-64176. (iii) The steps to –26 mV are overlaid. In A and B, voltage steps were 500 ms in duration, from a holding potential of –60 mV to –40 mV then increased in 2 mV steps. Steps from –40mV to –20 mV are shown in A and steps from –32 mV to –16 mV are shown in B. (C) (i) A P13 cell displaying a small hysteretic current in response to a voltage ramp command. (ii) The current hysteresis was enhanced with the application of FPL-64176, shown 6 min later and (iii) subsequently reduced with nimodipine, shown after an additional 7 min. Note that nimodipine application eliminated the inflection points during both the depolarizing and hyperpolarizing phases of the ramps, and shifted the apparent voltage of activation to the right (dotted line).

with the hysteretic current, then if L-type calcium channels are responsible for this current, it is not surprising that the application of nimodipine shifts this apparent activation voltage to the right (Fig. 4C).

In contrast to the dihydropyridines, acute application of ω-conotoxin-GVIA (6 μM) did not eliminate the current inflections (four out of four cells; Fig. 5A). Interestingly, following application of ω-conotoxin, the late-onset currents were activated to the same steady-state level and no longer exhibited a relationship to the command voltage level. This is similar to what was seen in the simulation containing only dendritic L-type channels (Fig. 3A). This effect was predicted by Müller & Lux (1993) and is thought to result from the regenerative activation of voltage-gated calcium channels in an unclamped region of the cell.

The acute effects of ω-agatoxin-TK (400 nM) were tested in six cells. In four cells the toxin did not block the dendritic currents while the total current amplitude was reduced (Fig. 5B). In one cell, the inflection point was abolished while in the last cell the ω-agatoxin rapidly produced a reduction but not block of the amplitude of the late-onset currents.

To rule out the possibility that acute application of the toxins did not allow sufficient time for the toxins to act, cells were incubated in ω-agatoxin TK (400 nM, $n = 2$) or ω-conotoxin GVIA (3 μM, $n = 1$; 6 μM, $n = 2$) for 30–70 min. Even after prolonged exposure to the toxins, late-onset currents were still observed.

In summary, the late-onset currents were not blocked by application of ω-conotoxin-GVIA in seven out of seven cells, or following application of ω-agatoxin-TK in six out of seven cells. In contrast, these currents demonstrated sensitivity to dihydropyridines in seven out of seven cells and FPL-64176 in two out of two cells. These pharmacological results support the hypothesis that the late-onset calcium currents are mediated by dihydropyridine-sensitive L-type calcium channels.

The effects of ω-conotoxin-GVIA (6 μM) and ω-agatoxin-TK (400 nM) were also tested on the hysteretic currents. Co-application of these toxins reduced the large inward current on the ascending limb

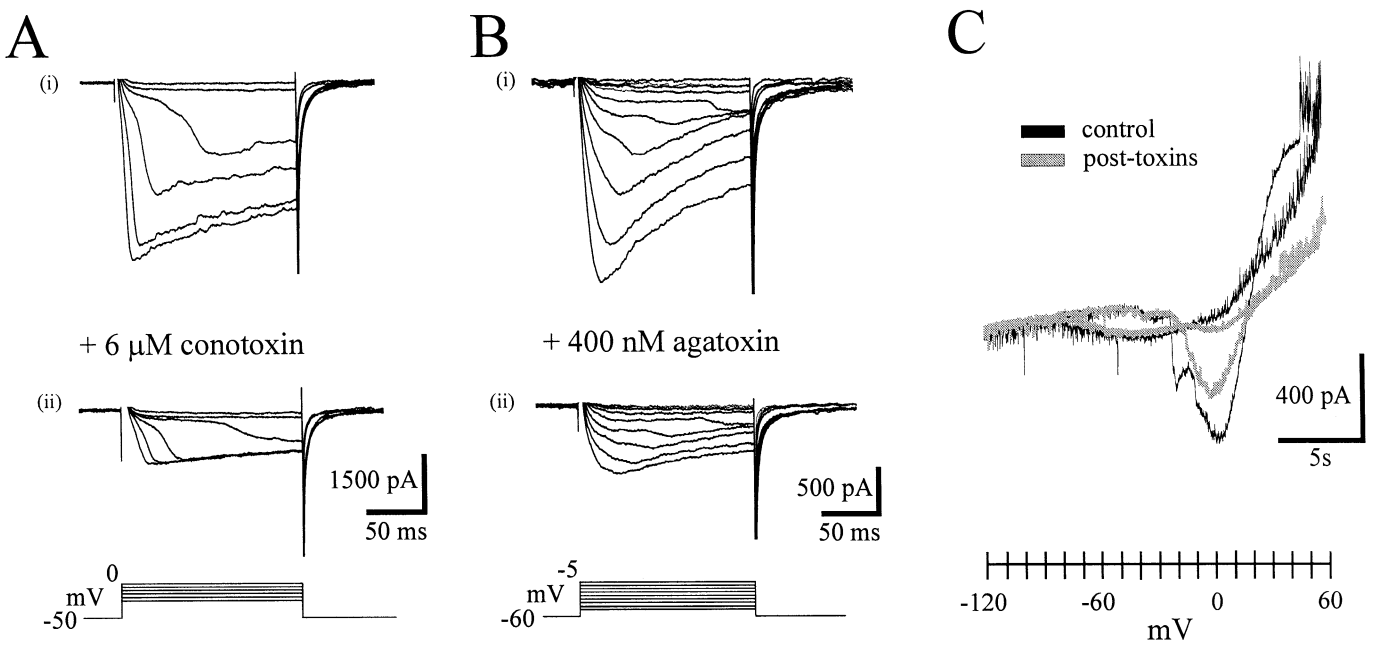

FIG. 5. The late-onset and hysteretic currents are not blocked by N- and P/Q-type channel blockers. (A) Addition of a saturating concentration of ω-conotoxin-GVIA reduced the total calcium current in this P15 motoneuron, but the dendritic currents were still evident. Note that the peak current remains constant at increasing voltage steps following toxin application. Holding potential of –50 mV with 150 ms × 5 mV steps from –25mV to 0 mV. (B) In this P12 motoneuron, addition of ω-agatoxin-TK reduced the total current without eliminating the late currents. Holding potential of –60 mV with 150 ms × 5 mV steps to –5 mV. Both A and B were in 1.5 mM calcium. (C) Overlaid current traces from a P10 motoneuron before (black) and approximately 3 min after (grey) application of 400 nM ω-agatoxin-TK and 6 μM ω-conotoxin-GVIA. A large reduction in the inward current that was elicited during the ascending phase of the ramp can be seen in the absence of any significant change in the hysteretic current.

of the ramp, indicating that there is an N- and/or P/Q-type component to this current. However, the hysteretic currents were not affected by these toxins ($n = 2$; Fig. 5C). This adds further support to the hypothesis that this current is mediated primarily by L-type channels.

Immunohistochemical localization of motoneuronal α_{1D} subunits

The presence of L-type calcium channels on motoneuron dendrites was examined with immunofluorescence using a polyclonal antibody to the α_{1D} subunit ($n = 4$ adult animals; three additional animals were studied using 3,3′-diaminobenzidine tetrahydrochloride immunohistochemistry, data not illustrated). Previous work demonstrated somatic and proximal dendritic labelling with the anti-α_{1C} antibody, and probable dendritic labelling using the anti-α_{1D} antibody (Jiang *et al*., 1999a). In this study, motoneuronal dendrites were examined for a distance of up to 300 μm from the cell soma. Punctate dendritic labelling of the α-$_{1D}$ subunit was seen typically after the second or third dendritic branch point, with less labelling proximal to this (Fig. 6). Given the absence of significant dendritic labelling of the α_{1C} subunit (Westenbroek *et al*., 1998; Jiang *et al*., 1999a), this leads to the suggestion that the dendritic L-type calcium channels responsible for the late-onset calcium currents are of class D.

Discussion

This study has demonstrated a dihydropyridine-sensitive calcium current (L-type) originating in the dendrites of spinal motoneurons in slices harvested from mice older than postnatal day 7. A similar current can be demonstrated in a motoneuron model by placing a low-voltage-activated non-inactivating current in the dendrites. Furthermore, the immunohistochemical labelling demonstrates class D L-type calcium channels in motoneuron dendrites.

Evidence for a dendritic calcium current

In the present study, the dendritic origin of the voltage-activated calcium currents is shown indirectly using somatic whole-cell recording, and combining this with results using both immunohistochemistry and modelling studies. There is little question that the recorded currents are mediated by calcium. Under the same experimental conditions it has been demonstrated that these currents are voltage dependent, sensitive to the extracellular calcium concentration and cadmium, and are sensitive to the specific channel blockers ω-agatoxin-TK, ω-conotoxin GVIA, dihydropyridines and FPL-64176 (Carlin *et al*. 2000). The ability of increased extracellular calcium concentrations to make distal currents more visible in the soma would be predicted because the raised calcium not only increases the membrane resistance but also the negative slope conductance (Figs 2B and 2C2; Müller & Lux, 1993).

In this study it was found that approximately one quarter of cells did not display either late-onset or hysteretic currents even with elevated extracellular calcium. There are a number of possible explanations for this, which cannot be distinguished in the current study. For example, it is possible that a subpopulation of motoneurons (e.g. subtype) do not possess these dendritic channels, and that these cells would have a different role in motor output than those cells that could express plateau potentials (see below). A second possibility is that the cells in which dendritic currents were not seen had a significant portion of their dendritic trees (and hence α_{1D} channels) removed by slicing.

Although some investigators have recorded calcium currents directly from dendrites (e.g. Magee & Johnston, 1995; Mouginot

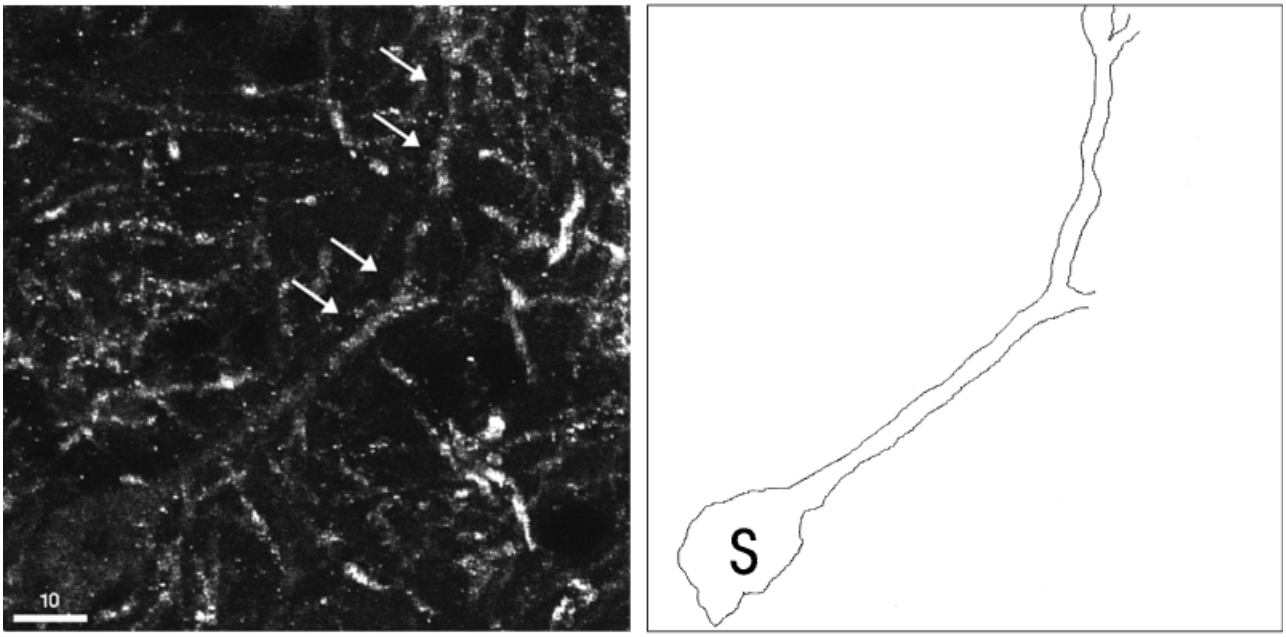

FIG. 6. Class D L-type channels were demonstrated in the dendrites of large ventral horn neurons using an anti-α_{1D} polyclonal antibody. Confocal look-through image from an adult mouse spinal cord slice (20 µm). The labelling was punctate-like, and increased distal to the second or third dendritic branch points (arrows) in this adult mouse spinal cord. An outline of the soma (S) and dendrites is shown on the right. Scale bar, 10 µm.

et al., 1997), it is unlikely that such an approach would be successful in the distal dendrites of motoneurons where these channels are probably located. On the other hand, recording dendritic calcium currents, or their resultant potential changes, with a somatically placed electrode has also been demonstrated previously. Destexhe *et al*. (1996) combined electrophysiology with a neuromorphic model to demonstrate LVA channels in the dendrites of thalamic reticular neurons. Hirst & McLachlan (1986) reported a late-onset calcium current in voltage clamped sympathetic chain cells. The current was concluded to originate in an electrically distant location due to the change in latency but not amplitude with increasing voltage steps. This is consistent with the experimental data presented here (e.g. Figure 5Aii).

The modelling data from Müller & Lux (1993) suggest that one can deduce the position of a spatially localized inward current from examination of the delay and rate of activation of the somatically recorded inward current. However, given the limited information regarding the properties of the channels from which this current originates, and the multiple types of calcium currents present, the position of the currents cannot be accurately determined from examination of the trajectory alone. Both the delay and the rate of activation of the late-onset current were variable and depended on the size of the voltage step (e.g. Figs 1A and 5A). Near 'threshold' for these currents, the delay to onset of the late current may be as long as several hundred milliseconds (e.g. Figure 4Ai). On first examination, such a delay may be difficult to explain based on the relatively electrically compact nature of motoneurons (Thurbon *et al*., 1998). However, Müller & Lux (1993) demonstrated delays of up to 2 time constants with conductances placed at 0.5–0.8 λ; the majority of cells displaying late-onset currents in this study had time constants < 60 msec. Furthermore, using current-clamp protocols in a two-compartment model, Booth *et al*. (1997) demonstrated that several-hundred-millisecond delays in onset of plateau potentials with current steps near the threshold of activation of the plateaux can be explained using dynamical systems theory. This theory predicts long delays to onset of plateaux near threshold (the onset voltage of the negative slope conductance), and then with increasing current steps, the delay will be shorter. This is similar to the data presented here in voltage clamp (Figs 2A, 4 and 5). This would explain why the long delays were more often seen with protocols using 2-mV increments in voltage commands, as the likelihood of a voltage step being close to the threshold (or 'saddle-node' in the terminology of dynamical systems theory) would be increased.

Another possible explanation for the delayed currents might be that the somatic channels are in equilibrium between 'reluctant' and 'willing' states (Bean, 1989). It could be argued that if the channel equilibrium in these cells in this preparation favours the reluctant state, and that if time in a depolarized state is required to shift to the willing state (Delgado-Lezama & Hounsgaard, 1999), then a late-onset current might be seen. This may in fact explain the 'wind-up' phenomenon previously reported in turtle motoneurons (Svirskis & Hounsgaard, 1997). Two observations make this possibility less likely. Firstly, it has not been possible to facilitate the total calcium current elicited by voltage steps from –60 to 0 mV following 75-ms prepulses to +100 mV in any of the 13 cells tested (Carlin *et al*. 2000). Secondly, during the hyperpolarizing phase of the voltage ramps there are two conspicuous peaks of inward current created by an inflection point in the current waveform (see Figs 1, 2B, 3C and 4C). It is suggested that this 'double hump' represents the separation of a somatic current, which is partly inactivating, and a dendritic current, which is seen as the hysteretic current. The inflection point between these humps indicates that the second (more hyperpolarized) hump must be created either by newly activating somatic channels or by persistently activated dendritic channels which become a current source for the soma as it is being hyperpolarized. The former possibility would seem unlikely given the absence of evidence that dihydropyridine-sensitive channels can activate (or reactivate) during a slow repolarization after a prolonged depolarization and then remain open to potentials as low as –100 mV. On the other hand, a more reasonable explanation for this 'double hump' would be that the apparent activation is due to the relative depolarization of the nonclamped dendrites, which persists as the soma is hyperpolarized. The more hyperpolarized somatic voltage

then acts as a 'sink' for the inward current mediated by noninactivating dendritic channels. This latter hypothesis is supported by the immunostaining of class D L-channels that are clearly separated from the soma.

Channel type underlying the dendritic currents

The dendritic currents shown here were consistently blocked by dihydropyridines and enhanced by FPL-64176 and are therefore mediated by L-type channels. Previous authors have demonstrated the presence of L-type calcium channels in mammalian spinal motoneurons but have not reported a dendritic calcium current (Mynlieff & Beam, 1992; Hivert *et al*., 1995; Gao & Ziskind-Conhaim, 1998; Scamps *et al*., 1998). These cells were either embryonic or neonatal, which may explain why dendritic L-type currents were not reported. This is consistent with the immunohistochemical observation that the α_{1D}-containing L-type channels develop in the first two postnatal weeks (Jiang *et al*., 1999a). In the present study, the use of older mice would have facilitated the detection of α_{1D}-mediated dendritic currents.

In addition to L-type calcium channels, it is possible that there are dendritic N- and/or P/Q-type channels as well. It can be seen in Fig. 5A and B that the slope of the late current decreases with the addition of conotoxin and agatoxin. Because the effects of channel rundown are difficult to distinguish in this situation, the possibility that N- and/or P/Q-type channels contribute to this current cannot be ruled out. Furthermore, the ability of agatoxin and conotoxin to block the spike-like current during the slow voltage ramp command (Fig. 5C) may indicate the presence of non-L-type channels in the unclamped dendrites. However, the facts that the late and hysteretic currents were not blocked with the application of saturating concentrations of these toxins and that the late currents were still seen in cells incubated in these toxins would indicate that the contribution of current mediated by non-L-type channels to the persistent inward dendritic current recorded in the soma (i.e. hysteretic current) was minimal compared with the current mediated by L-type calcium channels.

Voltage of activation of the dendritic current

As the recorded dendritic currents are remote from the patch electrode, the voltage of activation cannot be determined in the current study. Nevertheless, it is interesting to note that the somatic voltage of activation of the calcium currents is lower in the cells with dendritic/hysteretic currents than in those without. Furthermore, the modelling data demonstrated a similar lower apparent voltage of activation in the ramp studies in models with LVA channels (Fig. 3B). Interestingly, the voltage of activation of the inward current is –45 mV in the LVA model, and averages –47 mV in the experimental data.

Traditionally, the L-type calcium channels have been considered to belong to the HVA class of channels. However, in hippocampal pyramidal cells, dihydropyridine-sensitive channels have been found to activate at (Magee *et al*., 1996; Davies *et al*., 1999) or near (Avery & Johnston, 1996) resting potentials in physiological concentrations of calcium (2–2.5 mM). There is also evidence in support of LVA dihydropyridine-sensitive calcium channels in magnocellular neurosecretory cells of the supraoptic nucleus (Fisher & Bourque, 1996), and guinea pig trigeminal motoneurons (Del Hsiao *et al*., 1998). Previous studies have looked at either α_{1C} or α_{1D} channels in isolation, inserted into Xenopus embryos. In comparing these studies, it would seem that the threshold of activation of the α_{1D} channels is lower than that of the α_{1C} channels (compare Williams *et al*., 1992 fig. 6b with Tomlinson *et al*., 1993 figs 1b and 3). [Note that subunits other than the α_1 may have some modulatory effect on the voltage of activation (Tomlinson *et al*., 1993; Klugbauer *et al*., 1999).] With the immunohistochemical data supporting the dendritic dihydropyridine channels being of class D (whilst class C appear to be more proximal: Westenbroek *et al*., 1998; Jiang *et al*., 1999a), it could be speculated that these channels have a lower voltage of activation than the class C channels, and hence account for the findings presented in this study.

Implications for bistability

It has previously been suggested that a persistent dendritic current is responsible for the depolarizing drive underlying self-sustained repetitive firing in motoneurons, and that this current also underlies a second stable membrane potential at a level more depolarized than rest (hence the term 'bistability'). Experimental evidence supporting a dendritic location of this plateau current comes from a number of sources. Schwindt & Crill (1977) first demonstrated a region of negative slope conductance in cat motoneurons, which they attributed to a persistent (noninactivating) calcium current. In examining these data, Gutman (1991) convincingly argued that this current must be dendritic in origin because the firing continued even when the somatic voltage returned to resting potential. Furthermore, he pointed out that in their voltage-clamp data, the inward current persisted even after returning the soma to resting potential (Gutman, 1991; compare Lee & Heckman, 1996).

Plateau potentials were also demonstrated in cat motoneurons following systemic administration of monoamines, which were thought to unmask the inward current by blocking outward potassium currents (Conway *et al*., 1988). These potentials were studied further in turtle motoneurons, where they were shown to be sensitive to dihydropyridines (Hounsgaard & Kiehn, 1989). Furthermore, because of the morphology of these cells, application of electrical fields could differentially polarize the soma and dendrites, leading to experiments which demonstrated that the current underlying the plateau potential was dendritic in origin (Hounsgaard & Kiehn, 1993). Interestingly, the activation voltage of plateau potentials in the cat is lower during excitatory synaptic input than with intracellular somatic current injection, which is also consistent with a dendritic location of the plateau-mediating channels (Bennett *et al*., 1998).

Modelling studies simulating bistability also support a dendritic location of the persistent inward current underlying the plateau potential. Booth & Rinzel (1995) and Booth, Rinzel & Kiehn (1997) used a two-compartment model based on data from turtle motoneurons to model bistability. In order to reproduce the bistability seen in experiments, they found that it was essential for the somatic spike-generating mechanism to be electrically distant from (weakly coupled to) the conductance underlying the plateau current. This is supported by other models including those of motoneurons (Gutman, 1991) and Purkinje cells (De Jaeger *et al*., 1997).

It was previously reported that a motor rhythm in the whole isolated spinal cord becomes sensitive to dihydropyridines after postnatal day 7 and that L-type calcium channels are best demonstrated in motoneurons after this age (Jiang *et al*., 1999a). The present study demonstrates dendritic L-type currents in motoneurons after postnatal day 8. It is conceivable that with the development of these currents, motoneurons are able to produce plateau potentials which result in firing rates necessary for functional motor behaviours such as posture and locomotion – activities which mature at postnatal day 9 (Jiang *et al*., 1999b). In fact, during fictive locomotion in the adult cat, there is a voltage-dependent increase in the excitation of motoneurons by the spinal network for locomotion (Brownstone *et al*., 1994). Furthermore, motoneurons fire at high

rates when first recruited, with little change in these rates with somatic current injection (Brownstone *et al*., 1992). A possible explanation for these phenomena is that activation of voltage-activated calcium currents leads to bistability. The presence of a dendritically located calcium current such as the one demonstrated here would support this possibility. Preliminary data have demonstrated calcium-mediated plateau potentials in mature mouse motoneurons (Jiang *et al*., 1999c).

In summary, this study demonstrates a persistent dihydropyridine-sensitive calcium current in mouse motoneurons resulting from activation of dendritically located channels. This current may be low-voltage-activated, mediated via class D L-type channels, and is probably responsible for the bistable behaviour seen in motoneurons.

Acknowledgements

The authors thank Dr R. E. Burke for supplying the morphology of the cat motoneuron used in the modelling, Dr D. Nance for his expert assistance with confocal microscopy, Drs B. Schmidt, S. Shefchyk and D. McCrea for helpful suggestions on the manuscript, and Deborah Manchur, Mike Sawchuk and Jeremy Rempel for their technical assistance. This work was supported by the Medical Research Council of Canada, the Manitoba Health Research Council (MHRC) and the Amyotrophic Lateral Sclerosis Society of Canada. R.M.B. is an MHRC Scholar, K.P.C. is supported by MHRC and University of Manitoba Studentships and K.E.J. by a Rick Hansen Neurotrauma Postdoctoral Fellowship.

Abbreviations

HVA, high-voltage-activated; *I–V*, current–voltage; LVA, low-voltage-activated; R_a, access resistance; R_i, input resistance; R_m, membrane resistance; WCC, whole cell capacitance.

References

Avery, R.B. & Johnston, D. (1996) Multiple channel types contribute to the low-voltage-activated calcium current in hippocampal CA3 pyramidal neurons. *J. Neurosci.*, **16**, 5567–5582.

Bean, B.P. (1989) Neurotransmitter inhibition of neuronal calcium currents by changes in channel voltage dependence. *Nature*, **340**, 153–156.

Bennett, D.J., Hultborn, H., Fedirchuk, B. & Gorassini, M. (1998) Synaptic activation of plateaus in hindlimb motoneurons of decerebrate cats. *J. Neurophysiol.*, **80**, 2023–2037.

Booth, V. & Rinzel, J. (1995) A minimal, compartmental model for a dendritic origin of bistability of motoneuron firing patterns. *J. Comput. Neurosci.*, **2**, 299–312.

Booth, V., Rinzel, J. & Kiehn, O. (1997) Compartmental model of vertebrate motoneurons for Ca^{2+}-dependent spiking and plateau potentials under pharmacological treatment. *J. Neurophysiol.*, **78**, 3371–3385.

Brownstone, R.M., Jordan, L.M., Kriellaars, D.J., Noga, B.R. & Shefchyk, S.J. (1992) On the regulation of repetitive firing in lumbar motoneurones during fictive locomotion in the cat. *Exp. Brain Res.*, **90**, 441–455.

Brownstone, R.M., Gossard, J.P. & Hultborn, H. (1994) Voltage-dependent excitation of motoneurones from spinal locomotor centres in the cat. *Exp. Brain Res.*, **102**, 34–44.

Carlin, K.P., Jiang, Z. & Brownstone, R.M. (2000) Characterisation of calcium currents in functionally mature mouse spinal motoneurones. *Eur. J. Neurosci.*, **12**, 1624–1634.

Conway, B.A., Hultborn, H., Kiehn, O. & Mintz, I. (1988) Plateau potentials in alpha-motoneurones induced by intravenous injection of L-dopa and clonidine in the spinal cat. *J. Physiol. (Lond)*, **405**, 369–384.

Crone, C., Hultborn, H., Kiehn, O., Mazieres, L. & Wigstrom, H. (1988) Maintained changes in motoneuronal excitability by short-lasting synaptic inputs in the decerebrate cat. *J. Physiol. (Lond.)*, **405**, 321–343.

Cullheim, S., Fleshman, J.W., Glenn, L.L. & Burke, R.E. (1987a) Three-dimensional architecture of dendritic trees in type-identified alpha-motoneurons. *J. Comp. Neurol.*, **255**, 82–96.

Cullheim, S., Fleshman, J.W., Glenn, L.L. & Burke, R.E. (1987b) Membrane area and dendritic structure in type-identified triceps surae alpha motoneurons. *J. Comp. Neurol.*, **255**, 68–81.

Davies, P.J., Ireland, D.R., Martinez-Pinna, J. & McLachlan, E.M. (1999) Electrophysiological roles of L-type channels in different classes of guinea pig sympathetic neuron. *J. Neurophysiol.*, **82**, 818–828.

Delgado-Lezama, R. & Hounsgaard, J. (1999) Adapting motoneurons for motor behavior. In Binder, M.D. (ed.), *Peripherial and Spinal Mechanisms in the Neural Control. of Movement*. Prog. Brain Res., **123**, 57–63.

Destexhe, A., Contreras, D., Steriade, M., Sejnowski, T.J. & Huguenard, J.R. (1996) *In vivo*, *in vitro*, and computational analysis of dendritic calcium currents in thalamic reticular neurons. *J. Neurosci.*, **16**, 169–185.

Destexhe, A., Neubig, M., Ulrich, D. & Huguenard, J. (1998) Dendritic low-threshold calcium currents in thalamic relay cells. *J. Neurosci.*, **18**, 3574–3588.

Eken, T. & Kiehn, O. (1989) Bistable firing properties of soleus motor units in unrestrained rats. *Acta Physiol. Scand.*, **136**, 383–394.

Feldman, D.H., Olivera, B.M. & Yoshikami, D. (1987) Omega Conus geographus toxin: a peptide that blocks calcium channels. *FEBS Lett.*, **214**, 295–300.

Fisher, T.E. & Bourque, C.W. (1996) Calcium-channel subtypes in the somata and axon terminals of magnocellular neurosecretory cells. *Trends Neurosci*, **19**, 440–444.

Fleshman, J.W., Segev, I. & Burke, R.B. (1988) Electrotonic architecture of type-identified alpha-motoneurons in the cat spinal cord. *J. Neurophysiol.*, **60**, 60–85.

Gao, B.-X. & Ziskind-Conhaim, L. (1998) Development of ionic currents underlying changes in action potential waveforms in rat spinal motoneurons. *J. Neurophysiol.*, **80**, 3047–3061.

Gutman, A.M. (1991) Bistability of dendrites. *Int. J. Neural. Syst.*, **1**, 291–304.

Hines, M.L. & Carnevale, N.T. (1997) The NEURON simulation environment. *Neural Comput.*, **9**, 1179–1209.

Hirst, G.D. & McLachlan, E.M. (1986) Development of dendritic calcium currents in ganglion cells of the rat lower lumbar sympathetic chain. *J. Physiol. (Lond.)*, **377**, 349–368.

Hivert, B., Bouhanna, S., Diochot, S., Camu, W., Dayanithi, G., Henderson, C.E. & Valmier, J. (1995) Embryonic rat motoneurons express a functional P-type voltage-dependent calcium channel. *Int. J. Dev. Neurosci.*, **13**, 429–436.

Hounsgaard, J., Hultborn, H., Jespersen, B. & Kiehn, O. (1984) Intrinsic membrane properties causing a bistable behaviour of alpha-motoneurones. *Exp. Brain Res.*, **55**, 391–394.

Hounsgaard, J. & Kiehn, O. (1989) Serotonin-induced bistability of turtle motoneurones caused by a nifedipine-sensitive calcium plateau potential. *J. Physiol. (Lond.)*, **414**, 265–282.

Hounsgaard, J. & Kiehn, O. (1993) Calcium spikes and calcium plateaux evoked by differential polarization in dendrites of turtle motoneurones in vitro. *J. Physiol. (Lond.)*, **468**, 245–259.

Hsiao, C.F., Del Negro, C.A., Trueblood, P.R. & Chandler, S.H. (1998) Ionic basis for serotonin-induced bistable membrane properties in guinea pig trigeminal motoneurons. *J. Neurophysiol.*, **79**, 2847–2856.

Hultborn, H., Wigstrom, H. & Wangberg, B. (1975) Prolonged activation of soleus motoneurones following a conditioning train in soleus 1a afferents - a case for a reverberating loop? *Neurosci. Lett.*, **1**, 147–152.

Jaeger, D., De Schutter, E. & Bower, J.M. (1997) The role of synaptic and voltage-gated currents in the control of Purkinje cell spiking: a modeling study. *J. Neurosci.*, **17**, 91–106.

Jiang, Z., Rempel, J., Li, J., Sawchuck, M., Carlin, K.P. & Brownstone, R.M. (1999a) Development of L-type calcium channels and a nifedipine-sensitive motor activity in the postnatal mouse spinal cord. *Eur. J. Neurosci*, **11**, 3481–3487.

Jiang, Z., Carlin, K.P. & Brownstone, R.M. (1999b) An *in vitro* fnctionally mature mouse spinal cord preparation for the study of spinal motor networks. *Brain Res.*, **816**, 493–499.

Jiang, Z., Carlin, K.P. & Brownstone, R.M. (1999c) Plateau potentials and wind-up in mouse spinal motoneurones. *Soc. Neurosci. Abstr.*, **25**, 562.12.

Jonas, P., Bischofberger, J. & Sandkuhler, J. (1998) Corelease of two fast neurotransmitters at a central synapse. *Science*, **281**, 419–424.

Kiehn, O. & Eken, T. (1997) Prolonged firing in motor units: evidence of plateau potentials in human motoneurons? *J. Neurophysiol.*, **78**, 3061–3068.

Klugbauer, N., Lacinová, L., Marais, E., Hobom, M. & Hofmann, F. (1999) Molecular diversity of the calcium channel alpha2delta subunit. *J. Neurosci*, **19**, 684–691.

Lee, R.H. & Heckman, C.J. (1996) Influence of voltage-sensitive dendritic conductances on bistable firing and effective synaptic current in cat spinal motoneurons *in vivo*. *J. Neurophysiol.*, **76**, 2107–2110.

Lee, R.H. & Heckman, C.J. (1998a) Bistability in spinal motoneurons *in vivo*:

systematic variations in rhythmic firing patterns. *J. Neurophysiol.*, **80**, 572–582.

Lee, R.H. & Heckman, C.J. (1998b) Bistability in spinal motoneurons *in vivo*: systematic variations in persistent inward currents. *J. Neurophysiol.*, **80**, 583–593.

MacLean, J.N., Schmidt, B.J. & Hochman, S. (1997) NMDA receptor activation triggers voltage oscillations, plateau potentials and bursting in neonatal rat lumbar motoneurons *in vitro*. *Eur J. Neurosci*, **9**, 2702–2711.

Magee, J.C. & Johnston, D. (1995) Characterization of single voltage-gated Na^+ and Ca^{2+} channels in apical dendrites of rat CA1 pyramidal neurons. *J. Physiol. (Lond)*, **487**, 67–90.

Magee, J.C., Avery, R.B., Christie, B.R. & Johnston, D. (1996) Dihydropyridine-sensitive, voltage-gated Ca^{2+} channels contribute to the resting intracellular Ca^{2+} concentration of hippocampal CA1 pyramidal neurons. *J. Neurophysiol.*, **76**, 3460–3470.

McHanwell, S. & Biscoe, T.J. (1981) The sizes of motoneurons supplying hindlimb muscles in the mouse. *Proc. R Soc. Lond B Biol. Sci.*, **213**, 201–216.

Mouginot, D., Bossu, J. & Beat, H. (1997) Low-threshold Ca^{2+} currents in dendritic recordings from Purkinje cells in rat cerebellar slice cultures. *J. Neurosci.*, **17**, 160–170.

Müller, W. & Lux, H.D. (1993) Analysis of voltage-dependent membrane currents in spatially extended neurons from point-clamp data. *J. Neurophysiol.*, **69**, 241–247.

Mynlieff, M. & Beam, K.G. (1992) Characterization of voltage-dependent calcium currents in mouse motoneurons. *J. Neurophysiol.*, **68**, 85–92.

Randall, A. & Tsien, R.W. (1995) Pharmacological dissection of multiple types of Ca^{2+} channel currents in rat cerebellar granule neurons. *J. Neurosci*, **15**, 2995–3012.

Scamps, F., Valentin, S., Dayanithi, G. & Valmier, J. (1998) Calcium channel subtypes responsible for voltage-gated intracellular calium elevations in embryonic rat motoneurons. *Neuroscience*, **87**, 719–730.

Schwindt, P. & Crill, W.E. (1977) A persistent negative resistance in cat lumbar motoneurons. *Brain Res.*, **120**, 173–178.

Schwindt, P.C. & Crill, W.E. (1980) Properties of a persistent inward current in normal and TEA-injected motoneurons. *J. Neurophysiol.*, **43**, 1700–1724.

Streit, J. & Lux, H.D. (1989) Distribution of calcium currents in sprouting PC12 cells. *J. Neurosci.*, **9**, 4190–4199.

Svirskis, G. & Hounsgaard, J. (1997) Depolarization-induced facilitation of a plateau-generating current in ventral horn neurons in the turtle spinal cord. *J. Neurophysiol.*, **78**, 1740–1742.

Svirskis, G. & Hounsgaard, J. (1998) Transmitter regulation of plateau properties in turtle motoneurons. *J. Neurophysiol.*, **79**, 45–50.

Takahashi, T. & Berger, A.J. (1990) Direct excitation of rat spinal motoneurones by serotonin. *J. Physiol. (Lond.)*, **423**, 63–76.

Takahashi, T. (1990) Membrane currents in visually identified motoneurones of neonatal rat spinal cord. *J. Physiol. (Lond)*, **423**, 27–46.

Teramoto, T., Niidome, T., Miyagawa, T., Nishizawa, Y., Katayama, K. & Sawada, K. (1995) Two types of calcium channels sensitive to omega-agatoxin-TK in cultured rat hippocampal neurones. *Neuroreport.*, **6**, 1684–1688.

Thurbon, D., Luscher, H.R., Hofstetter, T. & Redman, S.J. (1998) Passive electrical properties of ventral horn neurons in rat spinal cord slices [corrected and republished with original paging, article originally printed in J Neurophysiol 1998 May; 79 (5): 2485–2502]. *J. Neurophysiol.*, **80**, 2485–2502.

Tomlinson, W.J., Stea, A., Bourinet, E., Charnet, P., Nargeot, J. & Snutch, T.P. (1993) Functional properties of a neuronal class C L-type calcium channel. *Neuropharmacology*, **32**, 1117–1126.

Westenbroek, R.E., Hoskins, L. & Catterall, W.A. (1998) Localization of Ca^{2+} channel subtypes on rat spinal motor neurons, interneurons, and nerve terminals. *J. Neurosci.*, **18**, 6319–6330.

Williams, M.E., Feldman, D.H., McCue, A.F., Brenner, R., Velicelebi, G., Ellis, S.B. & Harpold, M.M. (1992) Structure and functional expression of alpha 1, alpha 2, and beta subunits of a novel human neuronal calcium channel subtype. *Neuron*, **8**, 71–84.

Ziskind-Conhaim, L. (1988) Electrical properties of motoneurons in the spinal cord of rat embryos. *Dev. Biol.*, **128**, 21–29.